International Journal of Biological Macromolecules 94 (2017) 396–405

Contents lists available at ScienceDirect

International Journal of Biological Macromolecules

journal homepage: www.elsevier.com/locate/ijbiomac

Covalent immobilization of tyrosinase onto cyanuric chloride crosslinked amine-functionalized superparamagnetic nanoparticles: Synthesis and characterization of the recyclable nanobiocatalyst

Kourosh Abdollahi, Farshad Yazdani*, Reza Panahi

Chemistry & Chemical Engineering Research Center of Iran (CCERCI), P.O. Box 14335-186, Tehran, Iran

ARTICLE INFO

Article history:
Received 10 August 2016
Received in revised form 17 October 2016
Accepted 18 October 2016
Available online 19 October 2016

Keywords:
Tyrosinase
Covalent immobilization
Superparamagnetic nanoparticles
Cyanuric chloride
High loading capacity

ABSTRACT

Magnetic nanoparticles (MNPs) were synthesized using the chemical co-precipitation method. Then the nanoparticles were coated with silica via hydrolysis of tetraethyl orthosilicate using the sol-gel process. The silica coated magnetic nanoparticles were amine-functionalized with 3-aminopropyltriethoxysilane/ethanol solution. Subsequently, the nanoparticles were added to a solution of cyanuric chloride in tetrahydrofuran to synthesize cyanuric chloride-functionalized magnetic nanoparticles (Cy-MNPs). For covalent immobilization of tyrosinase, Cy-MNPs were added to a freshly prepared tyrosinase solution and the mixture was shaken. The FTIR spectra, as well as EDX, analysis proved the covalent immobilization of tyrosinase on the nanoparticles. The magnetic properties of tyrosinase-immobilized magnetic nanoparticles (tyrosinase-MNPs) were specified by VSM analysis. TEM images indicated that the most of the tyrosinase-MNPs had a semi-spherical shape with an average size of 17 nm. The synthesized nanoparticles had a high loading capacity of 194 mg tyrosinase/g nanoparticles with an immobilization yield of 69%. The optimum condition for both free and immobilized tyrosinase was found at pH 7.0 and 35 °C. The immobilized enzyme was active after treatment of the particles at various pHs and temperatures for 100 min. In addition, reusability of the immobilized enzyme was investigated and it was proved its suitability to be used for more than 7 cycles. Also, tyrosinase-MNPs remained about 70% of its initial activity after storing at 4 °C for 40 days. This nanobiocatalyst with interesting properties is promising for practical application in wastewater treatment and biosensor development.

1. Introduction

Enzymes are known as natural biocatalysts that catalyze chemical reactions in living organisms. They have several advantages compared with chemical catalysts such as high reaction rate under a mild pH and temperature, low energy consumption, toxicity and side reactions and high selectivity [1]. Therefore, enzymes are considered to be more effective than conventional catalysts [2]. Tyrosinase is an enzyme that belongs to oxidoreductase group with a copper-containing active center which can bind to oxygen molecules to oxidize several groups of phenolic and polyphenolic compounds to highly unstable o-quinones which are less toxic and insoluble [3–5].

Tyrosinase is responsible for numerous biological vital functions such as pigmentation, sclerotization, primary immune response and host defense. In fruits, vegetables and especially in commercial mushroom (*Agaricus bisporus*), this enzyme causes browning, a commercially unwelcome phenomenon. The active site of tyrosinase has a di-copper center. Three nitrogen atoms, coming from three adjacent histidine residues, coordinate each copper ion in the active site. Thus, three forms of met, oxy and deoxy can be experienced by the enzyme [6]. Also, tyrosinase exhibits two catalytic properties of monooxygenase and oxidase activities that occur consecutively. At the first step, the oxidation of monophenols by oxygen occurs as it passes through four enzyme states (E_{deoxy}, E_{oxy}, $E_{oxy\text{-}M}$ and $E_{met\text{-}D}$). In the second step, the enzyme passes through several enzyme states (E_{deoxy}, E_{oxy}, $E_{oxy\text{-}D}$, E_{met}, $E_{met\text{-}D}$) and oxidizes o-diphenols. O-quinones, which spontaneously react with each other to form oligomers, are formed as a result of the two cycles mentioned above [3,7]. However, the application of this enzyme in many fields of industry is often limited by some difficulties such as lack of operational stability and catalytic ability [8], the high price of the free enzyme, the existence of some contaminants such as laccase, β-glucosidase, β-xylosidase and xylanase found in almost

* Corresponding author.
E-mail address: fyazdani@ccerci.ac.ir (F. Yazdani).

http://dx.doi.org/10.1016/j.ijbiomac.2016.10.058
0141-8130/

all different commercial preparation of this enzyme, and problems related to its separation from the reaction medium [9–11].

Enzyme immobilization on different supports helps to overcome some of these limitations and can improve the operational stability, shelf life, the process of separation from the product and the reusability of enzyme [10–13]. Immobilization of tyrosinase on different solid carriers has been reported so far [14,15]. Covalent bonding is considered an efficient immobilization technique to improve the catalytic activity by stabilization of the active conformation [16,17]. However, improper bonding could also affect the active center of an enzyme, which may consequently decrease the enzymatic activity and efficiency. Therefore, it is still important to develop novel and appropriate methods for immobilization of enzymes. In recent years, magnetic nanoparticles have been considered potential carrier materials for the preparation of heterogeneous catalysts. The superior properties of magnetic nanostructured materials such as superparamagnetic behavior, low cost, high chemical and physical stability in a wide range of operational conditions, biocompatibility, low toxicity and eco-friendly characteristic, ease of separation and high capacity for loading biomacromolecules make them suitable to be used as supports for the immobilization of protein [17–24]. As an exclusive advantage, immobilized enzymes on magnetic nanoparticles (MNPs) can be easily separated from reaction media (such as wastewater treatment reactors) with the help of an external magnetic force. The experiments indicate the loading capacity of the carrier and its corresponding enzyme activity can be substantially increased by functionalizing the surface of magnetic nanoparticles with amino groups [21,25–27]. Chemical stability, high magnetization, biocompatibility and low coercivity are some requirements for all of the bioconjugation application of magnetic colloids. These requirements can be met by coating magnetic nanoparticles with silica. In this way, magnetic nanoparticles are protected by the outer shell of silica, which provides suitable bonding sites for modification of the nanoparticles surface with amino groups [28]. Various techniques have been proposed to prepare silica-coated superparamagnetic nanoparticles with core/shell structures by forming a silica shell on the surface of the pre-synthesized nanoparticles for immobilization of enzymes. Several results about preparation, characteristics and applications of immobilized enzymes on such a core – shell system have been presented in the literature [29]. Recently, cyanuric chloride (2, 4, 6-trichlorotriazine) has been used as a linker for immobilization of biomolecules and proteins due to its specific properties such as low price, chemical selectivity and biocompatibility. Nevertheless, this chemical compound has been seldom used for the functionalization of magnetic nanoparticles. This paper demonstrates an easy method for high loading immobilization of tyrosinase with high catalytic activity, thermal and pH stability and easy reusability using cyanuric chloride as the linker.

2. Materials and methods

2.1. Materials

For tyrosinase extraction, the fresh mushroom (*Agaricus bisporus*) was purchased from a local market. L-DOPA was obtained from Sigma-Aldrich. L-Tyrosinase, ferric chloride hexahydrate ($FeCl_3{\cdot}6H_2O$), ferrous chloride tetrahydrate ($FeCl_2{\cdot}4H_2O$), cyanuric chloride (Cy), ethanol (99.9%), ammonium sulfate, bovine serum albumin (BSA), coomassie brilliant blue G-250, tetraethyl orthosilicate (TEOS), ammonium hydroxide solution 25%, 3-aminopropyltriethoxysilane (APTES) and tetrahydrofuran (THF) were purchased from Merck. Other chemicals were analytical grade.

2.2. Enzyme extraction

Briefly, the fresh mushrooms (*Agaricus bisporus*) were cut into pieces and mixed with pre-cold acetone (−22 °C) for 30 min, then centrifuged for 20 min at 7000 rpm and 0 °C. Afterward, the pulp was separated and resuspended in phosphate buffer (pH 7.0), and the mixture was centrifuged at 10,000 rpm and 0 °C for 20 min. Protein impurities were salted out by adding ammonium sulfate powder to the supernatant to make a 30% saturated solution, and the mixture was stirred for 30 min at 0 °C. The supernatant was separated and adjusted to a saturation of 60% by adding the salt and stirred for 30 min at 0 °C. Subsequently, the mixture was centrifuged at 10,000 rpm for 20 min and the precipitate containing tyrosinase was dissolved in the phosphate buffer and stored at −22 °C [30]. The activity of free and immobilized tyrosinase was determined according to the method reported by Lu et al. [31] with some modifications using 1 mM L-tyrosine (cresolase activity) as substrate in phosphate buffer (pH 7, 0.05 M) at room temperature. The enzyme activity unit (U) is described as the amount of enzyme causing an increase of absorbance by 0.001/min at room temperature. Thus, 16.7 μL of the free enzyme was added to 550 μL of L-tyrosine solution, and the increase in absorbance was recorded at certain time intervals in order to determine free enzyme activity.

The amount of the enzyme loaded on MNPs was assayed by measuring the initial and final concentration of tyrosinase in the immobilization solution in accordance with the Bradford method using bovine serum albumin as standard [32]. The amount of enzyme that attached to MNPs was calculated from Eq. (1):

$$\text{Immobilizationefficiency}(\%) = [(C_i - C_f)/C_i] \times 100 \quad (1)$$

Where C_i is the initial concentration of tyrosinase and C_f is the concentration of unbound tyrosinase collected after washing the immobilized tyrosinase three times with phosphate buffer. The activity of the extracted tyrosinase was higher than 10000 U/mL. It was diluted to 4800 U/mL with a protein concentration of about 2.8 mg/mL, and the solution was used for the immobilization process.

2.3. Synthesis of magnetic nanoparticles

The chemical co-precipitation method, known as a simple and convenient procedure, was used to synthesize magnetic nanoparticles due to the literature with some modifications [33]. In order to prepare 0.1 M solutions of Fe^{3+} and Fe^{2+}, 0.5137 g of $FeCl_3{\cdot}6H_2O$ and 0.1889 g of $FeCl_2{\cdot}4H_2O$ were added to 19 mL and 9.5 mL deionized water, respectively. Then, both solutions were added to 150 mL deionized water that was previously deoxygenated by bubbling with N_2 for 10 min. The reaction was performed in a three-neck flask, equipped with mechanical stirrer and immersed in a 60 °C water bath, in the presence of a constant nitrogen flow. Afterward, 15 mL of 1 M NaOH solution was added drop by drop to the reaction solution. Stirring was continued for 5 min after complete addition of NaOH solution. The black precipitates were separated with a strong magnet and washed three times with 40 mL of deionized water.

2.4. Preparation of silica coated magnetic nanoparticles

Magnetic nanoparticles were coated with silica by hydrolysis of TEOS using the sol-gel method. The bare magnetic nanoparticles (0.22 g) were dispersed in 60 mL of ethanol and ultrasonicated for 10 min under a constant nitrogen flow. Then, 10 mL of deionized water, 4.5 mL of ammonium hydroxide solution and 0.6 mL of TEOS were added to the suspension and the mixture was stirred for 5 h at room temperature. The silica coated magnetic nanoparticles were

magnetically separated from the mixture and washed 3 times with ethanol and deionized water [34].

2.5. Surface modification of magnetic nanoparticles

To functionalize the surface of the prepared silica coated magnetic nanoparticles with the amino group, an adapted method was used [34]. First, the silica coated magnetic nanoparticles (200 mg) and APTES (1.5 mL) were added to 30 mL of ethanol in a round bottom flask and the suspension was stirred for 3 h at room temperature. Subsequently, the reaction was continued for 2 h at 50 °C. As prepared functionalized magnetite nanoparticles were separated by a strong magnet and washed thoroughly with ethanol and deionized water and dried under vacuum at 60 °C for 2 h. Then, the surface of the magnetic iron oxide/SiO_2 nanoparticles was functionalized with 2,4,6-trichlorotriazine [2]. Thus, 0.1 g of cyanuric chloride and 0.220 g of the dried magnetic iron oxide nanoparticles were added to 20 mL of dry THF, and the mixture was stirred by means of a mechanical stirrer at 0 °C for 2 h. The cyanuric chloride MNPs (Cy-MNPs) were magnetically collected from the mixture, washed several times with THF and dried under vacuum at 40 °C.

2.6. Immobilization of tyrosinase onto the modified magnetic iron oxide nanoparticles

For covalent immobilization of tyrosinase onto the Cy-MNPs, 5 mg of the functionalized cyanuric chloride magnetic nanoparticles was added to 1500 μL of phosphate buffer (0.05 M, pH 7.0) and sonicated for 30 s. Then, 500 μL of the freshly prepared tyrosinase solution (4800 U/mL) was added to the suspension, and the mixture was shaken at room temperature for 18 h. The as prepared tyrosinase-immobilized magnetic nanoparticles (tyrosinase-MNPs) were removed from the mixture with a strong magnet and washed three times with 1000 μL of phosphate buffer (0.05 M, pH 7.0). The activity of tyrosinase-MNPs was measured in accordance with the procedure mentioned above. To maintain the absorbance of the reaction product within the linear range of the spectrometer used in the experiment, an appropriate amount of immobilized tyrosinase was added to 550 μL of L-tyrosinase solution. The nanoparticles were magnetically separated in 2 min intervals, and the absorbance of the supernatant was recorded spectrophotometrically at 475 nm.

2.7. Effect of pH and temperature on tyrosinase activity

To evaluate temperature effect, the free and immobilized tyrosinase activities were measured at different temperatures (25, 35, 45 and 55 °C) and pH 7.0. Additionally, the substrate solutions at different pH (4.0, 5.0, 6.0, 7.0 and 8.0) and room temperature were individually used to evaluate the effects of pH on free and immobilized tyrosinase activities.

2.8. Stability of the immobilized tyrosinase

The pH stability was determined by incubating an adequate amount of the tyrosinase-MNPs in phosphate buffers at a pH range of 4.0-8.0 and room temperature for 2 h. The particles were separated and the immobilized enzyme activity was measured at pH 7.0 and room temperature. The temperature stability was specified by incubating the tyrosinase-MNPs in phosphate buffer at pH 7.0 and different temperatures ranging from 25 to 65 °C for 2 h. Similarly, the activity of the immobilized enzyme was determined.

2.9. Reusability test

Reusability tests of the immobilized tyrosinase were performed at different pHs and temperatures. For this purpose, 5 mg of the tyrosinase-MNPs was added to 550 μL of L-tyrosine in phosphate or citrate-phosphate buffer at different pHs (4.0, 5.0, 6.0, 7.0 and 8.0) and the activity of the immobilized enzyme was measured for each cycle. To check temperature effects on reusability, the immobilized tyrosinase was incubated in L-tyrosine solution (pH 7.0) at a temperature range of 25–55 °C, and the corresponding activities were measured. For running the next cycles, the immobilized enzyme was washed 3 times, with the 500 μL buffer solution and then the particles were added to the fresh substrate solution. Experiments were repeated for several cycles. The highest activity was considered as 100%, and the other activity values were reported relatively.

2.10. Dephenolization by tyrosinase-MNPs

In order to investigate the application of tyrosinase-MNPs in wastewater treatment, 5 mg of immobilized tyrosinase was added to an aqueous solution containing 100 mg/L phenol and the mixture was stirred. The sample was taken every 20 min and concentration of phenol was measured by the colorimetric method at 510 nm using 4-aminoantipyrine and potassium ferricyanide [35].

2.11. Kinetic study

The kinetic analysis of the enzyme was performed using the Michaelis–Menten model:

$$\upsilon = \frac{-ds}{dt} = \frac{\upsilon_{max} S}{K_m + S} \quad (2)$$

In Eq. (2), υ_{max}, S and K_m are the maximum rate of reaction, the concentration of substrate (L-DOPA), and the Michaelis–Menten constant respectively. The activity of the immobilized enzyme was determined using different concentrations of L-DOPA (as substrate) in 0.05 M phosphate buffer at pH 7.0 and 25 °C. Constants of the model, υ_{max}, and K_m were found by plotting the graph of activity versus the substrate concentration. The values of K_m and υ_{max} were calculated by non-linear fitting of the model to the experimental data.

2.12. Storage stability

To investigate the effect of immobilization on storage stability of the enzyme, both the free and immobilized tyrosinase were stored in 0.05 M phosphate buffer (pH 7.0) at 4 °C. The residual activities were assayed every 10 days for a period of 70 days.

2.13. Loading capacity of the modified magnetic nanoparticles

The protein loading capacity of the functionalized superparamagnetic iron oxide nanoparticles was investigated by immobilizing BSA with different concentrations (0.75, 1.5, 3 and 6 mg/mL) onto the particles according to the method described for tyrosinase immobilization. At the end of the immobilization process, the protein content in the solution was determined using the Bradford protein assay, and the amount of loaded protein on the carrier was calculated.

2.14. Characterization

X-ray powder diffraction (XRD) (Bruker D8 Advance, with Cu Kα radiation, λ = 0.154060 nm) of the dried samples with scanning range from 4° to 70° was used to identify the phase purity

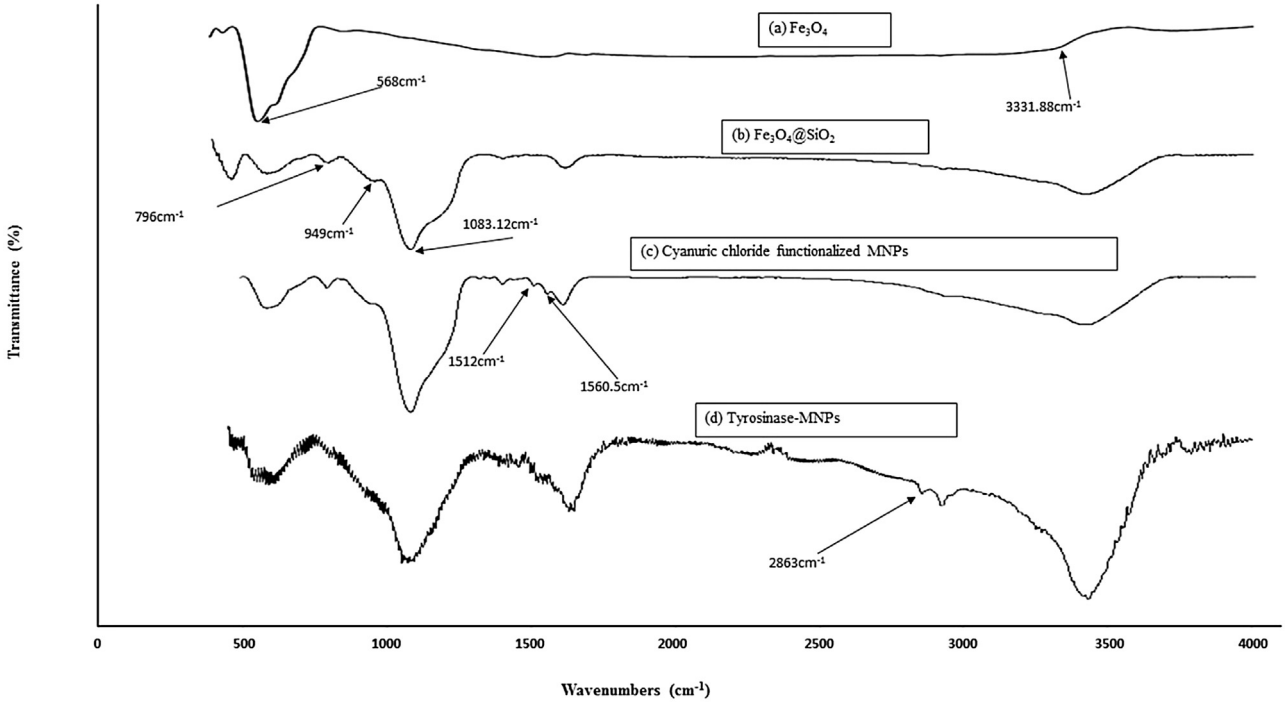

Fig. 1. FTIR analysis of (a) Fe_3O_4, (b) Fe_3O_4@SiO_2, (c) cyanuric chloride functionalized MNPs, and (d) tyrosinase-MNPs.

and crystal structure of the obtained magnetic nanoparticles. Size and morphology of the synthesized MNPs were studied using transmission electron microscopy (TEM), operating at 220 KV. Magnetization properties of the MNPs were analyzed using a vibrating sample magnetometer (VSM, Meghnatis Kavir Kashan Co., Iran). The EDX spectra were recorded by Scanning Electron Microscope (SEM) equipped with EDX detector (TESCAN Vega Model) to confirm successful immobilization of tyrosinase. The presence of surface functional groups and binding of the tyrosinase onto the modified surface magnetic nanoparticles were tested by FTIR spectroscopy (PERKIN-ELMER). Thermo-gravimetric analysis (TGA) was carried out on the dried powdered samples with a uniform heating rate of 10 °C/min and a temperature range of 200–800 °C under a high purity nitrogen atmosphere using a Netzsch – TGA 209F1 instrument.

3. Results and discussion

3.1. Characterization of nanoparticles

3.1.1. FT-IR

The Fourier transform infrared (FT-IR) spectra of the synthesized iron oxide NPs are shown in Fig. 1. The absorbance at 568 cm^{-1} is related to the Fe—O bond and the peak in 3331.88 cm^{-1} is ascribed to the H—O—H bond which is in harmony with the reported IR spectra for iron oxide NPs [36,37]. The silica coated magnetic iron oxide sample showed a strong band at 1083.12 cm^{-1} and two weak bands at 796 and 949 cm^{-1} corresponding to the stretching vibrations of (Si—O—Si), (Si—OH) and (Si—O—Fe), respectively [38]. Cyanuric chloride-functionalized magnetic nanoparticles sample showed two bands at 1512 cm^{-1} and 1560.5 cm^{-1} in the spectrum, supporting the successful binding of cyanuric chloride to the surface of modified magnetic nanoparticles. Compared to the FI-IR spectrum of Cy-Fe_3O_4, a new characteristic absorption peak appeared at 2863 cm^{-1} (C—H aliph bond) in the spectrum of tyrosinase-MNPs, which could demonstrate the successful immobilization of the enzyme onto modified core-shell magnetic nanoparticles [2].

3.1.2. EDX spectrum analysis

The EDX spectrum of the tyrosinase-MNPs indicated the presence of copper on the surface of magnetic nanoparticles (see Fig. 1 in Ref. [39]). The tyrosinase is a copper-containing enzyme, and this result confirms the successful immobilization of tyrosinase onto the cyanuric chloride functionalized magnetic nanoparticles.

3.1.3. Covalent binding of tyrosinase on Cy-MNPs

Based on the FTIR and EDX results, the schematic diagram for the preparation process of the Cy-MNPs as a carrier and tyrosinase-immobilized particles is represented in Fig. 2. The surface of silica coated MNPs was modified with APTES reagent to produce amino groups on the surface of iron oxide@SiO_2. Then, cyanuric chloride was used as an activating agent to prepare the modified MNPs for the covalent attachment of tyrosinase. Finally, tyrosinase was immobilized on the particles.

3.1.4. XRD analysis

In the XRD pattern of the prepared bare magnetic nanoparticles (see Fig. 2 in Ref. [39]) five specific peaks (2θ = 30.2°, 35.59°, 43.33°, 57.21°, and 62.58°) related to the corresponding indices of (220), (311), (400), (511) and (440) were observed respectively. It reveals that the prepared magnetic nanoparticles have cubic spinel structure according to the standard XRD data cards of magnetic iron oxide nanoparticles crystal (JCPDS No. 85-1436) [40,41]. In addition, the average size of the iron oxide nanoparticles was about 12 nm based on Debye–Scherrer's equation.

3.1.5. TEM analysis of tyrosinase-MNPs

The size and morphology of the tyrosinase-MNPs were characterized by the TEM method. The results confirmed that the dimension of tyrosinase-MNPs was in the nanometer range. The size distribution histogram and TEM images indicated that most of the particles had a spherical shape with an average size of 17 nm (see Fig. 3a and b in Ref. [39]). The smaller size of the tyrosinase-MNPs results in the higher specific surface area, and consequently it offers a higher yield of enzyme immobilization.

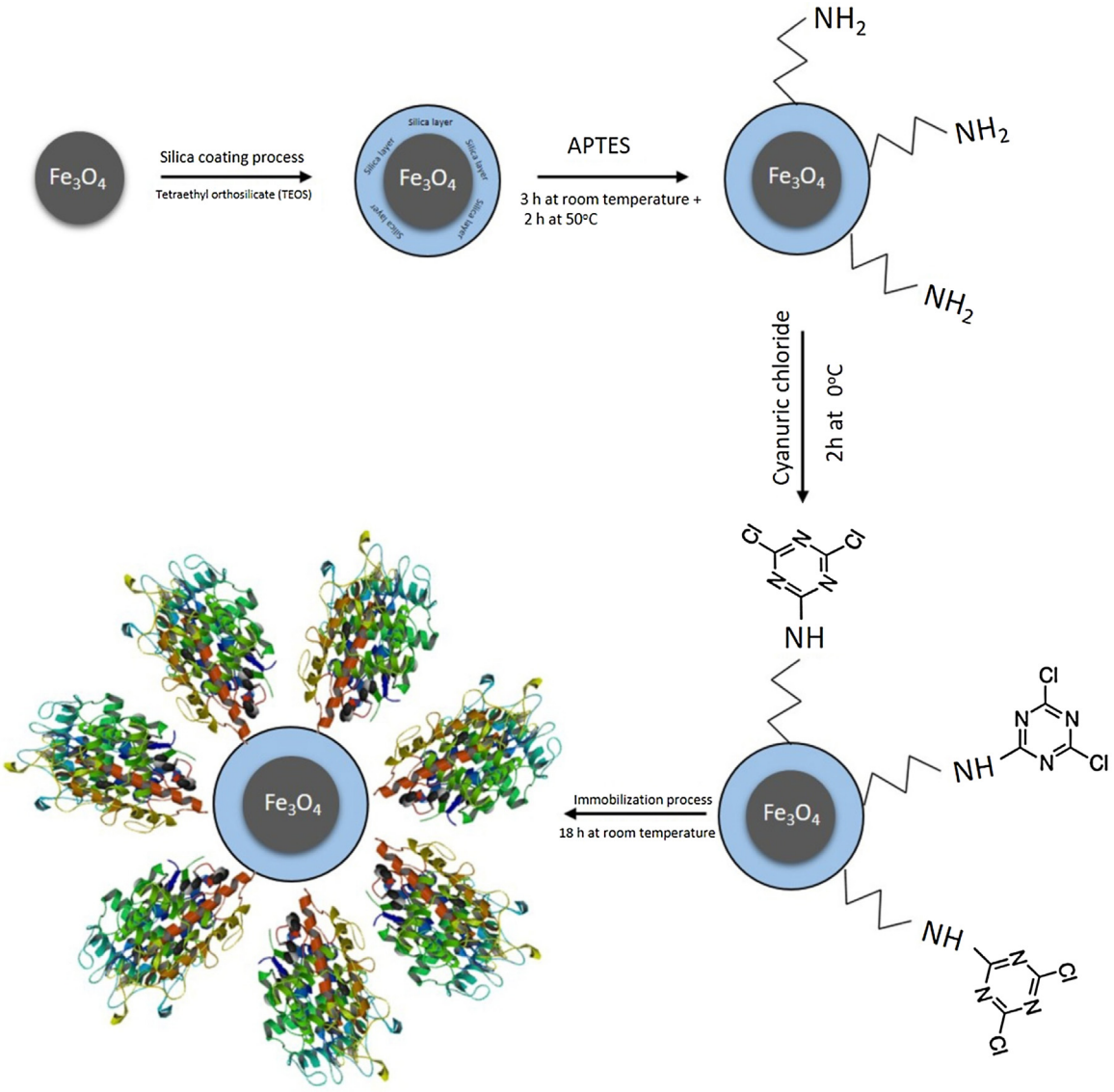

Fig. 2. Schematic representation of the nano-biocatalyst fabrication.

3.1.6. Vibrating sample magnetometer results

The magnetic properties of the bare magnetic nanoparticles, silica coated MNPs, and immobilized tyrosinase MNPs were investigated by using VSM at room temperature. The magnetization curves of these three samples are presented in Fig. 3. All the samples had a superparamagnetic behavior and saturation magnetization (Ms) of the bare iron oxide nanoparticles showed the high value of 51 emu/g. The Ms of iron oxide@SiO_2 and tyrosinase-MNPs were 25 and 17 emu/g, respectively. These lower Ms values are due to the formation of silica coating, functionalization of coated MNPs and enzyme immobilization. Furthermore, for investigating ease of magnetic separation of the prepared tyrosinase-MNPs, they were dispersed in an aqueous solution. It was observed that the suspended particles were easily separated from the solution in less than 1 min by means of an external magnet.

3.1.7. Thermo gravimetric analysis of the tyrosinase-MNPs

The weight loss diagram versus temperature of the cyanuric chloride functionalized magnetic nanoparticles and tyrosinase-MNPs were investigated (see Fig. 4 in Ref. [39]). For both Cy-MNPs and tyrosinase-MNPs, the first weight loss step was observed in the temperature range of 30–200 °C, which can be related to the elimination of physically absorbed water molecules on the surface of the samples. The weight loss of the Cy-MNPs sample from 200 to 800 °C was about 11.2% while that for the tyrosinase-MNPs, at the same temperature range, was about 27.4%. The difference between these two weight losses (about 16.2%) is attributed to the thermal decomposition of immobilized tyrosinase and confirms successful immobilization of tyrosinase on cyanuric chloride functionalized magnetic nanoparticles.

3.2. Immobilized tyrosinase characterization

3.2.1. Enzyme activity and loading capacity of the nanoparticles

Enzyme immobilization onto magnetic nanoparticles can improve the application of enzymes in industrial processes. The immobilized enzyme had an average activity of 189 U/g with an immobilization yield of 69% (194 mg/g nanoparticles). As shown in Table 1, the loading amount of tyrosinase onto Cy-MNPs was much higher than that of previous works. The high loading capacity of the particles can be attributed to the large surface area of the nanomaterials as well as the high reactivity of cyanuric chloride.

Table 1
Comparison of loading capacity of the different carries.

Enzyme	Carrier	Activating agent	Enzyme loading (mg/g)	Reference
Tyrosinase	Polymethylchloride styrene	Glutaraldehyde	4.17	[42]
Tyrosinase	Ca-Alginate beads	Epicholorhydrin	2.26	[43]
Tyrosinase	Glass beads	Cinnamoylated derivates of d-sorbitol	1.18	[44]
Tyrosinase	Magnetic beads	Glutaraldehyde	2.8	[45]
Tyrosinase	Microperl industrial glass beads	Hexacinnamate of d-sorbitol	1.18	[46]
Tyrosinase	Chitosan-Clay composite beads	Glutaraldehyde	26.8	[47]
Tyrosinase	Diatoms biosilica particles	Glutaraldehyde	37.1	[48]
Tyrosinase	Dry epoxy-silica	3-glycidoxypropyl trimethoxysilane(GPTMS)	30.23	[49]
Tyrosinase	Cy-MNPs	Cyanuric chloride	194	This work

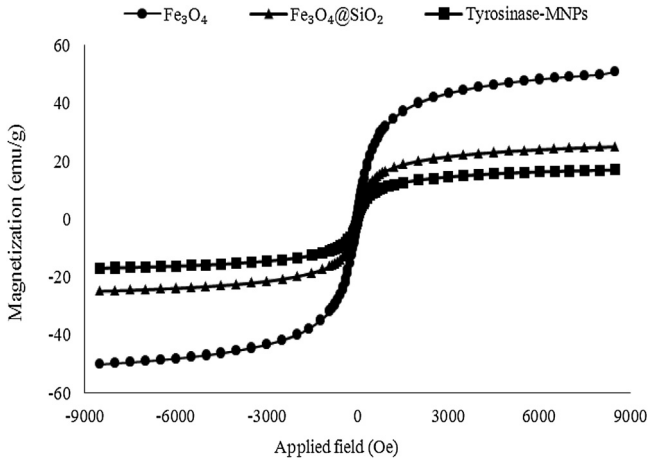

Fig. 3. Magnetization curves of (●) bare Fe_3O_4, (▲) Fe_3O_4@SiO_2, (■) Tyrosinase-Fe_3O_4 at room temperature.

Also, using another activating agent (cyanogen bromide) to immobilize other enzymes has been previously reported. For instance, the maximum loading capacity of immobilized invertase on chitosan using cyanogen bromide as an activating agent has been about 12 mg/g [50]. In other research, lipase and laccase have been immobilized on cyanogen–bromide–agarose support and cyanogen bromide Sepharose, respectively. In both studies, the loading amounts of the enzymes are lower than that of this work [51,52].

In addition, purification of extracted tyrosinase from mushroom *Agaricus bisporus* was performed (see Table 1 in Ref [39]). For this purpose, samples were taken during the extraction process and the corresponding activities and protein concentrations were measured. A slight increase in the specific activity occurred due to using the ammonium sulfate precipitation process to remove the fractional precipitation, mostly containing some contaminants from the final product. The final precipitate which had a fold purification of 1.7, was separated and dissolved in phosphate buffer as the final product.

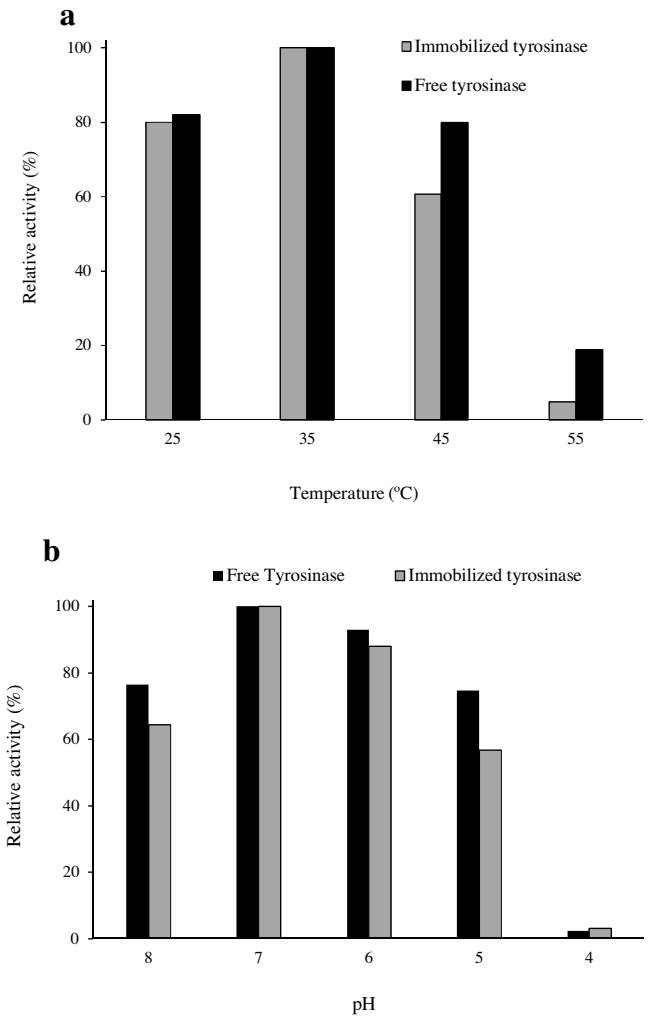

Fig. 4. Effect of temperature (a) and pH (b) on the activity of free and immobilized tyrosinase.

3.2.2. *Effects of pH and temperature on the enzyme activity and stability*

The effect of temperature on the activity of free and immobilized tyrosinase was assayed at pH 7.0 and different temperatures in a range of 25–55 °C. The highest activity of the free and immobilized enzyme was individually considered as 100%, and the activities at the other temperatures were reported proportional to the corresponding highest values. As seen in Fig. 4a, the highest activity of both immobilized and free tyrosinase occurred at 35 °C. By increasing the temperature from 35 to 55 °C, the activities of free and immobilized enzyme decreased because of enzyme deactivation at temperatures above 35 °C. The activity values of free and immobilized tyrosinase were also investigated in the pH range of 4.0–8.0. As shown in Fig. 4b, both free and immobilized enzymes showed considerably high activity at pH 7.0, while in the other pHs, the activity of both enzymes decreased. The lowest activity of free and immobilized tyrosinase was related to pH 4.0 with relative activities less than 5% which is attributed to the net positive charge of the enzyme at this condition, considering the pH value at the isoelectric point (pI) of tyrosinase is about 4.7 [53]. In another study concerning immobilization of tyrosinase on a polymeric membrane, the relative activities have found less than 25% and 45% at pH 5.0 and

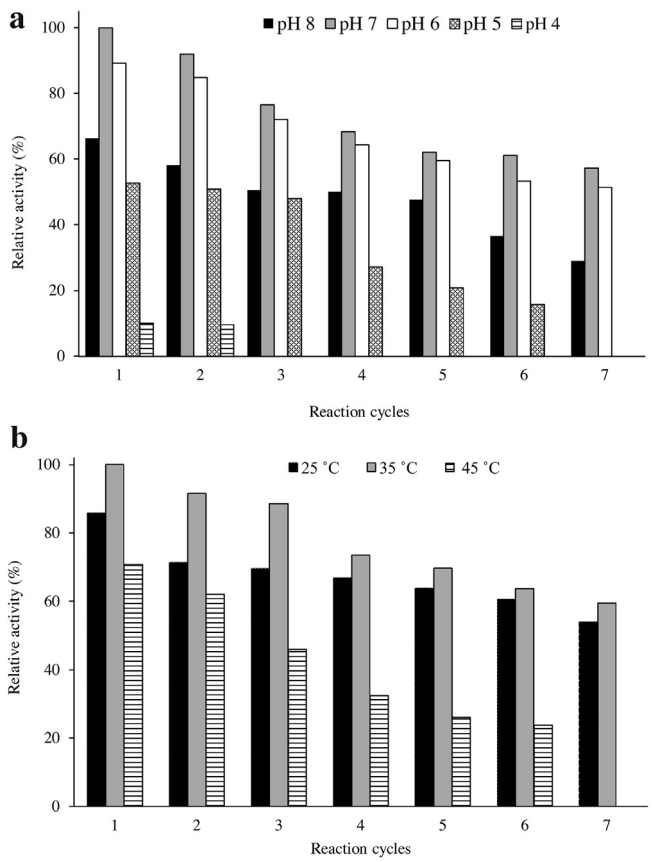

Fig. 5. Reusability test of immobilized tyrosinase at different (a) pHs and, (b) temperatures.

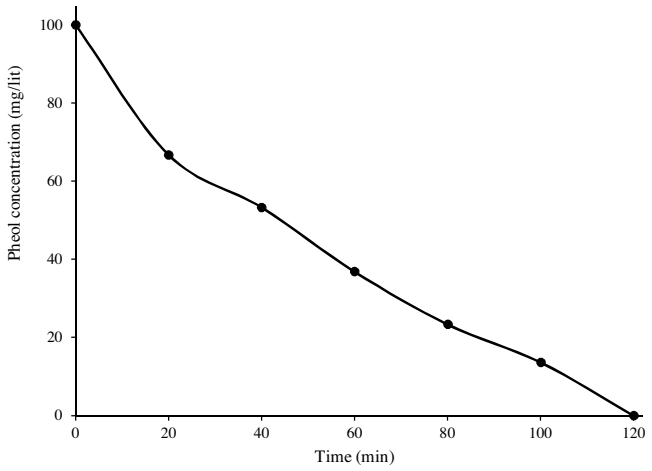

Fig. 6. Use of tyrosinase-MNPs for phenol elimination from an aqueous solution containing 100 mg/L phenol.

8.0 [9], while the corresponding values in this research were about 56% and 64%, respectively. These improvements are related to the stabilization of tyrosinase as a result of its covalent attachment on the surface of MNPs.

The tyrosinase stability could be affected by variation of pH and temperature too. Thus, the pH stability of immobilized tyrosinase was studied at different pHs (see Fig. 5a in Ref. [39]). The relative activity of immobilized tyrosinase was about 65.5% after incubation at pH 6.0 for 2 h. The immobilized enzyme was approximately stable after incubation of the enzyme for 100 min at pH 4.0, although after 2 h incubation, the activity loss was about 86%. The effect of temperature on immobilized tyrosinase stability was investigated by incubation of the enzyme at pH 7.0 and a temperature range of 35 to 65 °C (see Fig. 5b in Ref. [4]). The results showed that after 2 h incubation at 65 °C, immobilized enzymes almost had no activity which can be attributed to the thermal deactivation of tyrosinase at this temperature. Also, for incubation at 45 °C, the remaining activity of the immobilized enzyme reached about 40 and 12% after 100 and 120 min incubation, respectively. These results confirm the suitable stability of the immobilized tyrosinase in high temperatures and different pHs for about 100 min.

In addition, the apparent E_a of denaturation and Z-value were calculated using the results obtained from temperature stability experiments at different temperatures [54]. The values of Ea for denaturation and Z-value for tyrosinase-MNPs were about 38.35 kJ/mol and 52.9 °C, respectively. The low value of E_a for denaturation and high Z-value indicate the suitable stability of tyrosinase-MNPs at high temperatures. Generally, an increase in the conformational rigidity of enzymes structure and limiting susceptibility to drastic conformational changes can be achieved by enzyme immobilization on proper supports using appropriate procedures which make them suitable for industrial applications [55].

3.2.3. Reusability test of the immobilized tyrosinase

The reusability of tyrosinase-MNPs was tested at different temperatures (25–55 °C) and pHs (4.0–8.0) and the activity of the immobilized enzyme was measured. As shown in Fig. 5a, after a 7-cycle reuse at pH 7.0, the relative activity of immobilized tyrosinase was about 57%. However, the relative activity at pH 4.0 was less than 10% after 2 reaction cycles that can be related to the net positive charge of the immobilized tyrosinase as noted above. The investigation of temperature effect on reusability (Fig. 5b) confirmed that the best performance of immobilized tyrosinase occurred at 35 °C with a relative activity of 59% after the seventh cycle. The activity of tyrosinase-MNPs after reusing for 6 cycles at 45 °C was less than 25% so the experiment was not continued. This reduction in activity can be due to enzyme deactivation under this severe condition. These results indicate that tyrosinase-MNPs may be reused at least 7 cycles with appropriate levels of activities.

3.2.4. Phenol removal by tyrosinase-MNPs

The dephenolization capability of tyrosinase-MNPs was investigated by adding 5 mg of the immobilized tyrosinase to the phenolic solution and incubating the mixture at room temperature. As shown in Fig. 6, phenol was completely eliminated after 2 h. These results confirm the remarkable performance of the synthesized nanobiocatalyst in wastewater treatment.

3.2.5. Kinetic parameters

The activities of the immobilized and free enzyme at different substrate concentration were measured, and the Michaelis-Menten model was fitted to the corresponding results (Fig. 7). The values of K_m and υ_{max} were about 2.52 mM and 39880 U/mg for immobilized tyrosinase and also 1.14 mM and 62122 U/mL for free enzyme, respectively.

The K_m value for tyrosinase-MNPs was higher than that for free tyrosinase meaning that immobilized tyrosinase has a lower affinity for its substrates in comparison to the free one. This is related to the inherent characteristic of enzyme immobilization processes. The different affinities of the free and immobilized tyrosinase to the substrate are due to enzyme structural changes during the immobilization procedure [48], diffusional restrictions and introduction of steric hindrance formed by the support toward the active site causing the lack of adequate enzyme flexibility for binding of the natural

Table 2
A comparison of the kinetic constants of tyrosinase-MNPs and previous reports.

Enzyme	Carrier	K_m (mM)	υ_{max} (U/g)	Reference
Tyrosinase	Chitosan-Clay composite beads	1.7	568	[47]
Tyrosinase	Diatoms biosilica particles	2.59	1.98×10^4	[48]
Tyrosinase	Cy-MNPs	2.52	3.9880×10^7	This work

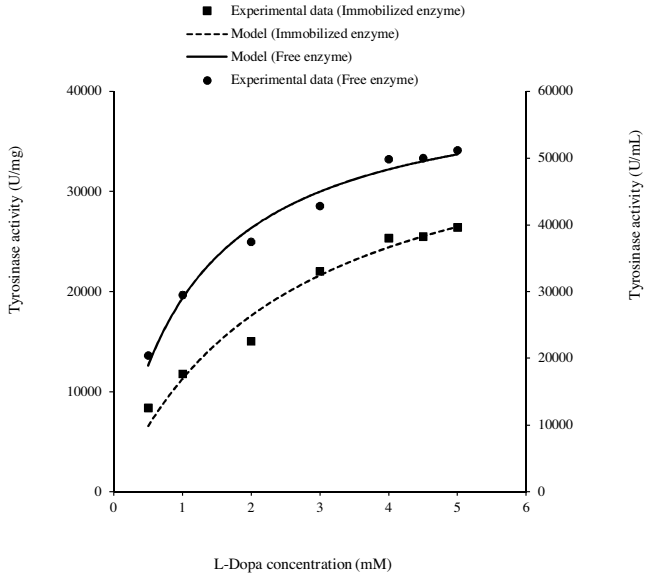

Fig. 7. Kinetic study of immobilized and free tyrosinase using different L-DOPA concentrations.

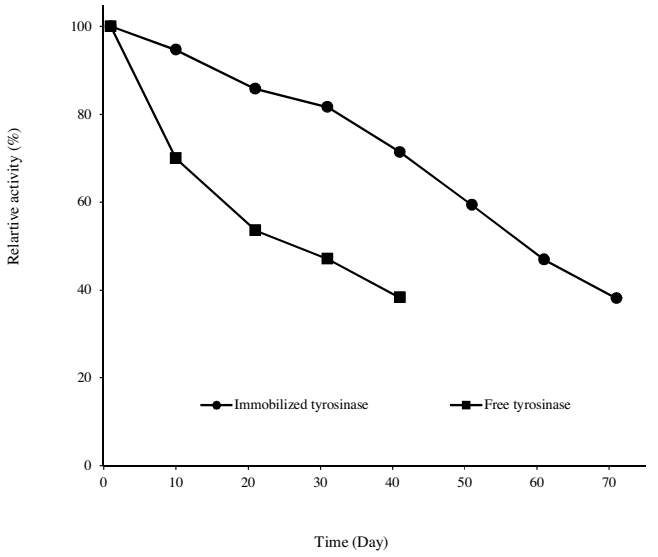

Fig. 8. Relative activities of the free and immobilized tyrosinase after storage at 4 °C.

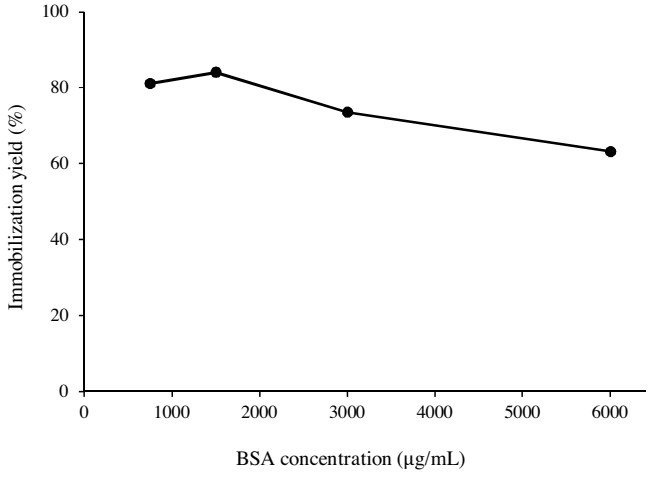

Fig. 9. Immobilization capacity of the cyanuric chloride functionalized MNPs by immobilizing different concentrations of BSA.

ligands during catalysis. Hence, the υ_{max} value of an immobilized enzyme is lower than that of a free enzyme.

In addition, as shown in Table 2, υ_{max} value of the tyrosinase-MNPs is surprisingly higher than those from the other studies. This can be attributed to the high amount of active tyrosinase immobilized onto the carrier, as a result of a large surface area of the nanoparticles and high reactivity of cyanuric chloride functionalized magnetic nanoparticles. Therefore, immobilization using this procedure with cyanuric chloride as an activating agent can improve kinetic parameters.

3.2.6. Storage stability

In order to investigate the storage stability of tyrosinase, the free and immobilized enzymes were stored at 4 °C for 70 days. As shown in Fig. 8, the immobilized enzyme had a relative activity of about 70% after storage for 40 days while that of the free enzyme was 40%. In addition, about 40% of the initial activity of immobilized tyrosinase remained after 70 days.

Immobilization significantly prevents this inherent loss of activity during storage. The relative activity of immobilized tyrosinase on modified diatom biosilica particles has been less than 60% after storage for about 40 days [48] while tyrosinase-MNPs showed better storage stability, indicating that immobilization improves the storage stability of tyrosinase.

3.2.7. Immobilization capacity of Cy-MNPs

BSA at different concentrations was immobilized on magnetic nanoparticles to find out the loading capacity of the nanoparticles (Fig. 9). The maximum immobilization yield of about 84% was obtained at a BSA concentration of 1500 μg/mL, and the yield decreased for the higher concentrations.

4. Conclusion

In this work, a new, easy, and inexpensive method for immobilization of tyrosinase onto magnetic nanoparticles using cyanuric chloride as an activating agent was reported. FTIR, EDX and TGA analyses confirmed that tyrosinase was covalently immobilized on cyanuric chloride functionalized MNPs. The synthesized nanoparticles had the high loading capacity of 194 mg protein/g nanoparticles with an immobilization yield of 69%. This notable capacity could be related to the large surface area of the nanomaterials as well as the high reactivity of cyanuric chloride modified nanoparticles. The best condition for catalytic activity of tyrosinase-MNPs was observed at pH 7.0 and 35 °C. The tyrosinase-MNPs

displayed proper stability at different temperatures and pHs. The reusability tests showed that the nano-biocatalyst was able to be reused at least 7 cycles with a relative activity of higher than 55%. In comparison with free enzyme, immobilized tyrosinase showed remarkable storage stability and kept almost 40% of its initial activity after 70 days. This nanobiocatalyst with interesting capacity, reusability, stability and shelf life is promising for practical application in wastewater treatment and biosensor development.

Acknowledgement

The authors would like to thank Prof. J.A. Nicell (Department of Civil Engineering and Applied Mechanics of McGill University, Canada) for his helpful comments.

References

[1] K. Min, Y.J. Yoo, Recent progress in nanobiocatalysis for enzyme immobilization and its application, Biotechnol. Bioprocess Eng. 19 (2014) 553–567.
[2] A. Soozanipour, A. Taheri-kafrani, A. Landarani, Covalent attachment of xylanase on functionalized magnetic nanoparticles and determination of its activity and stability, Chem. Eng. J. 270 (2015) 235–243.
[3] C.A. Ramsden, P.A. Riley, Tyrosinase: the four oxidation states of the active site and their relevance to enzymatic activation, oxidation and inactivation, Bioorg. Med. Chem. 22 (2014) 2388–2395.
[4] K. Ikehata, J.A. Nicell, Characterization of tyrosinase for the treatment of aqueous phenols, Bioresour. Technol. 74 (2000) 191–199.
[5] S. Rangelov, J.A. Nicell, A model of the transient kinetics of laccase-catalyzed oxidation of phenol at micromolar concentrations, Biochem. Eng. J. 99 (2015) 1–15.
[6] A.A. Saboury, S. Zolghadri, K. Haghbeen, A.A. Moosavi-Movahedi, The inhibitory effect of benzenethiol on the cresolase and catecholase activities of mushroom tyrosinase, J. Enzyme Inhib. Med. Chem. 21 (2006) 711–717.
[7] S. Mukherjee, B. Basak, Potential use of polyphenol oxidases (PPO) in the bioremediation of phenolic contaminants containing industrial wastewater, Rev. Environ. Sci. Biotechnol. 12 (2013) 61–73.
[8] N.M. Mahmoodi, M. Arabloo, J. Abdi, Laccase immobilized manganese ferrite nanoparticle: synthesis and LSSVM intelligent modeling of decolorization, Water Res. 67 (2014) 216–226.
[9] L. Donato, C. Algieri, A. Rizzi, L. Giorno, Kinetic study of tyrosinase immobilized on polymeric membrane, J. Memb. Sci. 454 (2014) 346–350.
[10] E. Mar, F. Rojas-melgarejo, F. Garc, P.A. Garc, Direct immobilization of tyrosinase enzyme from natural mushrooms (Agaricus bisporus) on d −sorbitol cinnamic ester, J. Biotechnol 126 (2006) 295–303.
[11] A. Rescigno, P. Zucca, A. Flurkey, J. Inlow, W.H. Flurkey, Identification and discrimination between some contaminant enzyme activities in commercial preparations of mushroom tyrosinase, Enzyme Microb. Technol. 41 (2007) 620–627.
[12] K. Labus, I. Gancarz, J. Bryjak, Immobilization of laccase and tyrosinase on untreated and plasma-treated cellulosic and polyamide membranes, Mater. Sci. Eng. C. 32 (2012) 228–235.
[13] D. Xu, J. Chen, Z. Yang, Use of cross-linked tyrosinase aggregates as catalyst for synthesis of l −DOPA, Biochem. Eng. J. 63 (2012) 88–94.
[14] S. Nadifiyine, M. Haddam, J. Mandli, S. Chadel, C.C. Blanchard, J.L. Marty, A. Amine, Amperometric biosensor based on tyrosinase immobilized on to a carbon black paste electrode for phenol determination in olive oil, Anal. Lett. 46 (2013) 2705–2726.
[15] N. Karim, H. Jin, Amperometric phenol biosensor based on covalent immobilization of tyrosinase on Au nanoparticle modified screen printed carbon electrodes, Talanta 116 (2013) 991–996.
[16] C. Cheng, K.C. Chang, Development of immobilized cellulase through functionalized gold nano-particles for glucose production by continuous hydrolysis of waste bamboo chopsticks, Enzyme Microb. Technol. 53 (2013) 444–451.
[17] J. Long, A. Jiao, B. Wei, Z. Wu, Y. Zhang, X. Xu, Z. Jin, A novel method for pullulanase immobilized onto magnetic chitosan/Fe_3O_4 composite nanoparticles by in situ preparation and evaluation of the enzyme stability, J. Mol. Catal. B Enzym. 109 (2014) 53–61.
[18] H. Ni, X. Sun, Y. Li, C. Li, Solvothermal self-assembly of magnetic Fe_3O_4 nanochains by ethylenediamine functionalized nanoparticles for chromium (VI) removal, J. Mater. Sci. 50 (2015) 4270–4279.
[19] A. Khalafi-Nezhad, M. Nourisefat, F. Panahi, L-Cysteine functionalized magnetic nanoparticles (LCMNP): a novel magnetically separable organocatalyst for one-pot synthesis of 2-amino-4H-chromene-3-carbonitriles in water, Org. Biomol. Chem. 13 (2015) 7772–7779.
[20] L. Xie, R. Jiang, F. Zhu, H. Liu, Application of functionalized magnetic nanoparticles in sample preparation, Anal. Bioanal. Chem. 406 (2013) 377–399.
[21] X. Shi, W. Gu, B. Li, N. Chen, Enzymatic biosensors based on the use of metal oxide nanoparticles, Microchim. Acta 181 (2014) 1–22.
[22] F. Yazdani, B. Fattahi, N. Azizi, Synthesis of functionalized magnetite nanoparticles to use as liver targeting MRI contrast agent, J. Magn. Magn. Mater. 406 (2016) 207–211.
[23] Y. Liu, S. Jia, Q. Wu, J. Ran, W. Zhang, S. Wu, Studies of Fe_3O_4-chitosan nanoparticles prepared by co-precipitation under the magnetic field for lipase immobilization, CATCOM 12 (2011) 717–720.
[24] P. Díez, R. Villalonga, M.L. Villalonga, J.M. Pingarrón, Supramolecular immobilization of redox enzymes on cyclodextrin-coated magnetic nanoparticles for biosensing applications, J. Colloid Interface Sci. 386 (2012) 181–188.
[25] C. Beladiya, R.K. Tripathy, P. Bajaj, G. Aggarwal, A.H. Pande, Expression, purification and immobilization of recombinant AiiA enzyme onto magnetic nanoparticles, Protein Express. Purif. 113 (2015) 56–62.
[26] M. Raita, J. Arnthong, V. Champreda, N. Laosiripojana, Modification of magnetic nanoparticle lipase designs for biodiesel production from palm oil, Fuel Process. Technol. 134 (2015) 189–197.
[27] Y. Huang, Y. Xi, Y. Yang, Degradation of 2, 4-dichlorophenol catalyzed by the immobilized laccase with the carrier of Fe_3O_4@MSS–NH_2, Chin. Sci. Bull. 59 (2014) 509–520.
[28] A. Morel, S.I. Nikitenko, K. Gionnet, A. Wattiaux, J. Lai-kee-him, C. Labrugere, B. Chevalier, G. Deleris, C. Petibois, A. Brisson, M. Simonoff, I. Bordeaux, L.H. Vigneau, A. Faculte, Sonochemical approach to the synthesis of Fe_3O_4@SiO_2 core-shell nanoparticles with tunable properties, ACS Nano 2 (2008) 847–856.
[29] J. Lee, Y. Lee, J.K. Youn, H. Bin Na, T. Yu, H. Kim, S. Lee, Y. Koo, J.H. Kwak, H.G. Park, H.N. Chang, M. Hwang, J. Park, J. Kim, T. Hyeon, Simple synthesis of functionalized superparamagnetic magnetite/silica core/shell nanoparticles and their application as magnetically separable high-performance biocatalysts, Small 4 (2008) 143–152.
[30] K. Zynek, J. Bryjak, M. Polakovič, Effect of separation on thermal stability of tyrosinase from Agaricus bisporus, J. Mol. Catal. B Enzym. 66 (2010) 172–176.
[31] L. Lu, M. Zhao, Y. Wang, Immobilization of laccase by alginate −chitosan microcapsules and its use in dye decolorization, Word J. Microbiol. Biotechnol. 23 (2007) 159–166.
[32] M.M. Bradford, A rapid and sensitive method for the quantitation microgram quantities of protein utilizing the principle of protein-dye binding, Anal. Biochem. 72 (1976) 248–254.
[33] Y. Jin, F. Liu, C. Shan, M. Tong, Y. Hou, Efficient bacterial capture with amino acid modified magnetic nanoparticles, Water Res. 50 (2013) 124–134.
[34] E. Ranjbakhsh, A.K. Bordbar, M. Abbasi, A.R. Khosropour, E. Shams, Enhancement of stability and catalytic activity of immobilized lipase on silica-coated modified magnetite nanoparticles, Chem. Eng. J. 179 (2012) 272–276.
[35] J. Yang, Y. Huang, Y. Yang, H. Yuan, X. Liu, Cagelike mesoporous silica encapsulated with microcapsules for immobilized laccase and 2, 4-DCP degradation, J. Environ. Sci. 38 (2015) 52–62.
[36] H. Veisi, J. Gholami, H. Ueda, P. Mohammadi, M. Noroozi, Magnetically palladium catalyst stabilized by diaminoglyoxime-functionalized magnetic Fe_3O_4 nanoparticles as active and reusable catalyst for Suzuki coupling reactions, J. Mol. Catal. A Chem. 396 (2015) 216–223.
[37] M. Nasr-esfahani, S.J. Hoseini, M. Montazerozohori, R. Mehrabi, H. Nasrabadi, Magnetic Fe_3O_4 nanoparticles: efficient and recoverable nanocatalyst for the synthesis of polyhydroquinolines and Hantzsch 1 4-dihydropyridines under solvent-free conditions, J. Mol. Catal. A Chem. 382 (2014) 99–105.
[38] Y. Chen, Z. Xiong, L. Zhang, J. Zhao, Q. Zhang, L. Peng, W. Zhang, M. Ye, H. Zou, Facile synthesis of zwitterionic polymer-coated core-shell magnetic nanoparticles for highly specific capture of N-linked glycopeptides, Nanoscale 7 (2015) 3100–3108.
[39] K. Abdollahi, F. Yazdani, R. Pahani, Data in support of covalent attachement of tyrosinase onto cyanuric chloride crosslinked magnetic nanoparticels, Data in brief, submitted.
[40] R.K. Gautam, P.K. Gautam, S. Banerjee, S. Soni, S.K. Singh, M.C. Chattopadhyaya, Removal of Ni(II) by magnetic nanoparticles, J. Mol. Liq. 204 (2015) 60–69.
[41] F. Yazdani, M. Edrissi, Effect of pressure on the size of magnetite nanoparticles in the coprecipitation synthesis, Mater. Sci. Eng. B Solid-State Mater. Adv. Technol. 171 (2010) 86–89.
[42] P.Y. Ho, M.S. Chiou, A.C. Chao, Production of L-dopa by tyrosinase immobilized on modified polystyrene, Appl. Biochem. Biotechnol. 111 (2003) 139–152.
[43] A. Yahşi, F. Şahin, G. Demirel, H. Tümtürk, Binary immobilization of tyrosinase by using alginate gel beads and poly (acrylamide-co-acrylic acid) hydrogels, Int. J. Biol. Macromol. 36 (2005) 253–258.
[44] M.E. Marín-Zamora, F. Rojas-Melgarejo, F. García-Cánovas, P.A. García-Ruiz, Effects of the immobilization supports on the catalytic properties of immobilized mushroom tyrosinase: a comparative study using several substrates, J.Biotechnol 131 (2007) 388–396.
[45] S. Tuncagil, S.K. Kayahan, G. Bayramoglu, M.Y. Arica, L. Toppare, L-Dopa synthesis using tyrosinase immobilized on magnetic beads, J. Mol. Catal. B Enzym. 58 (2009) 187–193.
[46] M.E. Marín-Zamora, F. Rojas-Melgarejo, F. García-Cánovas, P.A. García-Ruiz, Production of o-diphenols by immobilized mushroom tyrosinase, J.Biotechnol 139 (2009) 163–168.
[47] A. Dinçer, S. Becerik, T. Aydemir, Immobilization of tyrosinase on chitosan-clay composite beads, Int. J. Biol. Macromol. 50 (2012) 815–820.

[48] G. Bayramoglu, A. Akbulut, M. Yakup Arica, Immobilization of tyrosinase on modified diatom biosilica: enzymatic removal of phenolic compounds from aqueous solution, J. Hazard. Mater. 244–245 (2013) 528–536.
[49] K.B. de Oliveira, K.L. Mischiatti, J.D. Fontana, B.H. De Oliveira, Tyrosinase immobilized enzyme reactor: development and evaluation, J. Chromatogr. B Anal. Technol. Biomed. Life Sci. 945–946 (2014) 10–16.
[50] H.J. Hsieh, P.C. Liu, W.J. Liao, Immobilization of invertase via carbohydrate moiety on chitosan to enhance its thermal stability, Biotechnol. Lett. 22 (2000) 1459–1464.
[51] A.G. Cunha, G. Fernández-Lorente, J.V. Bevilaqua, J. Destain, L.M.C. Paiva, D.M.G. Freire, R. Fernández-Lafuente, J.M. Guisán, Immobilization of Yarrowia lipolytica lipase—a comparison of stability of physical adsorption and covalent attachment techniques, Appl. Biochem. Biotechnol. 146 (2008) 49–56.
[52] V. Addorisio, F. Sannino, C. Mateo, J.M. Guisan, Oxidation of phenyl compounds using strongly stable immobilized-stabilized laccase from Trametes versicolor, Process Biochem. 48 (2013) 1174–1180.
[53] P. Rijiravanich, K. Aoki, J. Chen, W. Surareungchai, M. Somasundrum, Micro-cylinder biosensors for phenol and catechol based on layer-by-layer immobilization of tyrosinase on latex particles: theory and experiment, J. Electroanal. Chem. 589 (2006) 249–258.
[54] P. Zucca, E. Sanjust, M. Loi, F. Sollai, M. Ballero, M. Pintus, A. Rescigno, Isolation and characterization of polyphenol oxidase from Sardinian poisonous and non-poisonous chemotypes of Ferula communis (L.), Phytochemistry 90 (2013) 16–24.
[55] A.A. Homaei, R.H. Sajedi, R. Sariri, S. Seyfzadeh, R. Stevanato, Cysteine enhances activity and stability of immobilized papain, Amino Acids 38 (2010) 937–942.